Published in IET Control Theory and Applications
Received on 23rd February 2009
Revised on 5th May 2009
doi: 10.1049/iet-cta.2009.0095

ISSN 1751-8644

Design of reduced-order nonlinear observers for energy conversion applications

A.E. Leon J.A. Solsona

Departamento de Ingeniería Eléctrica y de Computadoras, Instituto de Investigaciones en Ingeniería Eléctrica (IIIE) 'Alfredo Desages', Universidad Nacional del Sur (UNS), 1253 Alem Avenue, Bahía Blanca, PO 8000, Argentina
E-mail: aleon@gmail.com

Abstract: Here a systematic technique to design a reduced-order nonlinear observer for estimating signals in application to energy conversion systems is introduced. This observer presents a linear error dynamics in estimated variables and it is built in a methodical way. The proposed method has been motivated by problems arising in power conversion systems, but its use can be extended to other areas. The introduced observer is able to simplify the design of observer-based algorithms applied in power conversion systems. Examples are presented to show the advantages of the proposed method.

1 Introduction

State, parameter and disturbance estimation is frequently used in model-based controllers [1–3], feedforward disturbance compensators [4], variable monitoring and fault detection [5–7] among other applications. High-performance controllers based on state feedback and time-varying parameter compensation are used in many circuits and systems appearing in engineering applications [8–12]. A problem arising in practice is associated with the availability of sensors needed to implement a control law or a specific algorithm. Many times, the number of sensors must be reduced, because of either economic or technical reasons [13, 14]. In such cases, a fixed number of variables are measured and the others are estimated via an adequate technique [15]. Therefore the control strategy is implemented by using both measurements and estimates (examples of this kind of strategy can be found in [16–18]).

In [17], the above technique is proposed for controlling DC/DC converters. There, flatness theory is used to design a nonlinear controller and a feedforward compensator of the estimated load power is included to improve the converter performance. The used estimation technique results in time-varying error dynamics. Nevertheless, it must be remarked that the design of controllers for nonlinear systems based on observers with either time-varying or nonlinear error dynamics is complex. It is because separation theorem [19] does not work such as in the linear case. In the linear case, closed-loop stability (observer-based controller plus plant) is guaranteed by using the separation theorem. Consequently, the control law and observer convergence rate can be fixed independently. Since the separation theorem does not apply in the nonlinear case, when choosing the observer gains, some conditions should be considered to guarantee stability. Some researchers establish sufficient conditions to guarantee asymptotic convergence in the nonlinear case [20–24]. In [24], conditions are presented in order to establish how fast must the observer convergence be to guarantee closed-loop stability. For this reason, from the convergence rate point of view, it is preferable to construct observers with linear error dynamics in variables to be estimated, since estimation error trajectories are known exactly during the convergence transient, being easier the observer design and guaranteeing stability.

Many techniques were proposed to design nonlinear observers, for instance [25–29] to name just a few. Several techniques often used to design nonlinear observers can be found in [30, 31] and references there. These approaches obtain observer gains for stabilising the linear part of the system or a transformated system version, and then high-gain methods are used to keep the nonlinear part bounded. On the other hand, observers with linear error dynamics have been presented by some authors [32–35]. In these

cases, when certain conditions are verified, linear error dynamics is guaranteed by applying a nonlinear state coordinate transformation. Although the linear error dynamics is attained in transformed coordinates, generally the error dynamics is nonlinear when it is expressed in original coordinates. As mentioned, it is more advantageous to obtain linear error dynamics in variables to be estimated. For this reason, this work is addressed to the design of a reduced-order nonlinear observer in a systematic manner, with linear error dynamics in the original coordinates.

The paper is organised as follows. In Section 2, a motivating example is presented. Then, in Section 3, a systematic way of designing reduced-order nonlinear observers with linear error dynamics in original coordinates is introduced. In Section 4, more application examples are presented. Finally, conclusions are drawn in Section 5.

2 Motivating example

Consider the problem of constructing an observer to estimate a constant power load, p_{L}, in a DC–DC boost converter (Fig. 1), whose electrical model is given by

$$L\dot{i}_{\mathrm{dc}} = -(1-\eta)v_{\mathrm{dc}} + V_{\mathrm{in}} \tag{1}$$

$$C_{\mathrm{dc}}\dot{v}_{\mathrm{dc}} = (1-\eta)i_{\mathrm{dc}} + \frac{p_{\mathrm{L}}}{v_{\mathrm{dc}}} \tag{2}$$

where i_{dc} is the current of the DC-DC boost converter (A), v_{dc} the capacitor voltage (V), p_{L} the load power (W), V_{in} the input voltage (V), L the circuit inductance (H), C_{dc} the circuit capacitance (F) and η the control input.

In order to solve this problem, observers were introduced in [17, 18]. These observers are full order and reduced order, respectively, presenting time-varying error dynamics and state variable dependency. However, as previously mentioned, it is generally hard to design controllers for nonlinear systems based on observers with either time-varying or nonlinear error dynamics. From the convergence rate point of view, it is preferable to construct observers with linear error dynamics, since error trajectories are predictable. Although p_{L} is nonlinearly related with one of the states (v_{dc}), it is possible to construct an observer with linear error dynamics in original coordinates. To this end, it is possible proceed as follows. Choose the output

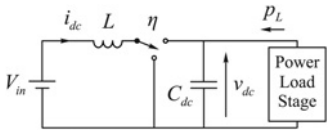

Figure 1 *Electrical circuit of a DC–DC boost converter*

transformation

$$w_1 = T(v_{\mathrm{dc}}) = \frac{1}{2}C_{\mathrm{dc}}v_{\mathrm{dc}}^2 \tag{3}$$

and construct the following reduced-order observer

$$\dot{\xi} = -\lambda\xi - \lambda((1-\eta)i_{\mathrm{dc}}v_{\mathrm{dc}} + \lambda w_1) \tag{4}$$

$$\hat{p}_{\mathrm{L}} = \xi + \lambda w_1 \tag{5}$$

In such a case, the linear estimation error dynamics becomes,

$$\dot{e} = -\lambda e \tag{6}$$

where $e \triangleq p_{\mathrm{L}} - \hat{p}_{\mathrm{L}}$ and λ is a constant design parameter fixing the convergence rate.

Many times power converters drive loads modeled as resistances (or conductances, G_{L}). In this case, the output transformation needed to construct a reduced-order nonlinear observer with linear error dynamics results

$$w_2 = T(v_{\mathrm{dc}}) = C_{\mathrm{dc}} \ln v_{\mathrm{dc}} \tag{7}$$

and the observer structure becomes

$$\dot{\xi} = -\lambda\xi - \lambda\left(\frac{(1-\eta)i_{\mathrm{dc}}}{v_{\mathrm{dc}}} + \lambda w_2\right) \tag{8}$$

$$\hat{G}_{\mathrm{L}} = \xi + \lambda w_2 \tag{9}$$

Remark 1: As will be demonstrated in the next section, this kind of observers have exponential convergence rate in original coordinates. This feature simplifies construction of closed- and open-loop algorithms when estimated variables are included.

Remark 2: These observers are based on nonlinear output transformations (w_1 and w_2), and they must be chosen to obtain linear error dynamics. For this reason, it is desirable to introduce a systematic method to design this kind of observer. In the next section, a systematic technique is presented. Later, others applications of the proposed technique will be introduced.

3 Systematic nonlinear observer design

3.1 Reduced-order nonlinear observer structure

Consider a class of nonlinear system given by

$$\dot{\mathbf{x}} = \mathbf{F}(\mathbf{x}_a, \mathbf{u})\mathbf{x} + \mathbf{g}(\mathbf{x}_a, \mathbf{u}) \tag{10}$$

where $\mathbf{x} \in \mathbb{R}^{n\times 1}$ is the state vector and $\mathbf{u} \in \mathbb{R}^{m\times 1}$ is the input vector, with $\mathbf{F} \in \mathbb{R}^{n\times n}$ and $\mathbf{g} \in \mathbb{R}^{n\times 1}$. The state vector is partitioned as $\mathbf{x} = [\mathbf{x}_a\ \mathbf{x}_b]^{\mathrm{T}}$, where $\mathbf{x}_a \in \mathbb{R}^{n_a\times 1}$ contains

measurable variables and $\mathbf{x}_b \in \mathbb{R}^{n_b \times 1}$ contains unmeasurable variables.

Although (10) represents a particular class of nonlinear systems, many circuits and systems can be modelled by this equation (see examples in the next sections). This representation can be rewritten as follows

$$\begin{bmatrix} \dot{\mathbf{x}}_a \\ \dot{\mathbf{x}}_b \end{bmatrix} = \begin{bmatrix} \mathbf{N}(\mathbf{x}_a, \mathbf{u}) & \mathbf{M}(\mathbf{x}_a, \mathbf{u}) \\ \mathbf{R}(\mathbf{x}_a, \mathbf{u}) & \mathbf{S}(\mathbf{x}_a, \mathbf{u}) \end{bmatrix} \begin{bmatrix} \mathbf{x}_a \\ \mathbf{x}_b \end{bmatrix} + \begin{bmatrix} \mathbf{g}_a(\mathbf{x}_a, \mathbf{u}) \\ \mathbf{g}_b(\mathbf{x}_a, \mathbf{u}) \end{bmatrix} \tag{11}$$

Now, the system given by (11) can be partitioned into two subsystems, resulting in

$$\dot{\mathbf{x}}_a = \mathbf{N}\mathbf{x}_a + \mathbf{M}\mathbf{x}_b + \mathbf{g}_a \tag{12}$$

$$\dot{\mathbf{x}}_b = \mathbf{R}\mathbf{x}_a + \mathbf{S}\mathbf{x}_b + \mathbf{g}_b \tag{13}$$

Define $\mathbf{T}: \mathbb{R}^{n_a} \mapsto \mathbb{R}^{p}$ a transformation depending on the measured variables

$$\mathbf{w} = \mathbf{T}(\mathbf{x}_a) \tag{14}$$

where $\mathbf{w} \in \mathbb{R}^{p \times 1}$. Then, differentiating (14) with respect to time results

$$\dot{\mathbf{w}} = \frac{\partial \mathbf{T}}{\partial \mathbf{x}_a}(\mathbf{N}\mathbf{x}_a + \mathbf{M}\mathbf{x}_b + \mathbf{g}_a) \tag{15}$$

From (15), it is possible to write

$$\mathbf{y} = \mathbf{C}\mathbf{x}_b \tag{16}$$

where the following definitions apply

$$\mathbf{y} \triangleq \dot{\mathbf{w}} - \frac{\partial \mathbf{T}}{\partial \mathbf{x}_a}(\mathbf{N}\mathbf{x}_a + \mathbf{g}_a) \tag{17}$$

$$\mathbf{C} \triangleq \frac{\partial \mathbf{T}}{\partial \mathbf{x}_a}\mathbf{M} \tag{18}$$

Equation (13) describes the dynamics of the unmeasured variables and (16) works as an output equation of the new subsystem. Therefore, a Luenberger-like reduced-order observer structure can be used to estimate the unmeasured variables $\mathbf{x}_b$. In this way

$$\dot{\hat{\mathbf{x}}}_b = \underbrace{\mathbf{S}\hat{\mathbf{x}}_b + \mathbf{R}\mathbf{x}_a + \mathbf{g}_b}_{\text{prediction term}} + \underbrace{\mathbf{G}(\mathbf{y} - \mathbf{C}\hat{\mathbf{x}}_b)}_{\text{correction term}} \tag{19}$$

where $\mathbf{G} \in \mathbb{R}^{n_b \times p}$ is the observer gain matrix. The correction term [see (19)] allows to fix the convergence rate of the estimation error and to reject parametric uncertainties and unmodelled dynamics appearing in the prediction term. Uncertainty attenuation is directly proportional to the $\mathbf{G}$ norm. Nevertheless, the maximum value of the $\mathbf{G}$ norm to be chosen is bounded by the noise of the measurements.

Replacing (17) and (18) in (19) results

$$\dot{\hat{\mathbf{x}}}_b = \mathbf{A}_r\hat{\mathbf{x}}_b + \mathbf{B}_r + \mathbf{G}\dot{\mathbf{w}} \tag{20}$$

where it was defined

$$\mathbf{A}_r \triangleq \mathbf{S} - \mathbf{G}\frac{\partial \mathbf{T}}{\partial \mathbf{x}_a}\mathbf{M} \tag{21}$$

$$\mathbf{B}_r \triangleq \mathbf{R}\mathbf{x}_a + \mathbf{g}_b - \mathbf{G}\frac{\partial \mathbf{T}}{\partial \mathbf{x}_a}(\mathbf{N}\mathbf{x}_a + \mathbf{g}_a) \tag{22}$$

As formulated, $\mathbf{x}_b$ estimation needs the $\mathbf{w}$ time-derivative [see (20)] to be implemented. However, the algorithm can be reformulated to avoid the amplification of noise appearing because of the measured variable differentiation. To this end, a transformation is applied. By defining

$$\boldsymbol{\xi} \triangleq \hat{\mathbf{x}}_b - \mathbf{G}\mathbf{w} \tag{23}$$

where $\boldsymbol{\xi} \in \mathbb{R}^{n_b \times 1}$, whereas its time-derivative becomes

$$\dot{\boldsymbol{\xi}} = \dot{\hat{\mathbf{x}}}_b - \mathbf{G}\dot{\mathbf{w}} \tag{24}$$

Finally, by rewriting (20) and considering (24), the observer structure is given by

$$\dot{\boldsymbol{\xi}} = \mathbf{A}_r(\boldsymbol{\xi} + \mathbf{G}\mathbf{w}) + \mathbf{B}_r \tag{25}$$

$$\hat{\mathbf{x}}_b = \boldsymbol{\xi} + \mathbf{G}\mathbf{w} \tag{26}$$

This equation describes a reduced-order observer because only the unknown variables ($\mathbf{x}_b$) are estimated. Reduced-order observers allow to diminish the computational burden and the peaking phenomenon influence [36].

Thus, it is possible to construct a reduced-order observer implementing (25) and (26), where $\mathbf{w} = \mathbf{T}(\mathbf{x}_a)$ is still to be chosen. This transformation will be designed in the next subsection in order to obtain a linear estimation error dynamics.

3.2 Linear error dynamics design

The estimation error defined as $\mathbf{e} = \mathbf{x}_b - \hat{\mathbf{x}}_b$ is analysed in the following lines. The estimation error dynamics is obtained by subtracting (19) from (13), consequently

$$\dot{\mathbf{e}} = \dot{\mathbf{x}}_b - \dot{\hat{\mathbf{x}}}_b = (\mathbf{S} - \mathbf{G}\mathbf{C})(\mathbf{x}_b - \hat{\mathbf{x}}_b) = \mathbf{A}_r\mathbf{e} \tag{27}$$

Equation (27) shows that the error dynamics is characterised by the matrix $\mathbf{A}_r$ (21). This equation is key for the development of the proposed method. By solving the partial differential equation (PDE) from (21), it is possible to find the transformation $\mathbf{T}$ needed to obtain a constant desired matrix $\mathbf{A}_r$. Where, the PDE will be solved if the observability conditions are verified, taking into account the available measurements for each particular application. When $\mathbf{A}_r$ is a constant matrix, the error dynamics is exponentially

doi: 10.1049/iet-cta.2009.0095

convergent with fixed convergence rate. Note that the exponential converge occurs in error original coordinates. Finally, it must be remarked that linear techniques can be used to assign the constant eigenvalues of $\mathbf{A}_r$.

4 Application to energy conversion systems

Many times, signals, parameters and disturbances must be estimated in engineering systems, as it is needed: (i) to variable monitoring, (ii) to design model-based high-performance controllers with a reduced number of sensors, (iii) to compensation of parametric uncertainties (for instance, due to skin and temperature effect, saturation or component modifications), (iv) to reject disturbance effects and (v) to detect and isolate faults. Among others, variables to be estimated in energy conversion applications are electrical resistances, load torques, electric power and converter losses. Generally, variables to be estimated are related in a nonlinear way, then it is convenient to construct nonlinear estimators instead of linear estimators which only perform well near to the linearised point. In these cases, we proposed to use a reduced-order nonlinear observer with linear error dynamics, due to this kind of observer presents a predictable transient response in the signal to be estimated.

In the signal monitoring case or detection and isolation of faults the choice of the exponential convergence rate of the estimation error, given by the $\mathbf{G}$ matrix or the λ constant in the scalar case, is designed as a trade-off between convergence speed and measurement noise amplification. The lesser the noise in sensors exists, the higher can be the observer gain, presenting a faster observer convergence. However, in case of use of the estimated signals in a closed-loop controller, an additional item must be taken into account when the observer gains are designed. In the linear case, closed-loop stability (observer-based controller plus plant) is guaranteed by using the separation theorem. Consequently, the control law and observer convergence rate can be fixed independently. Since the separation theorem does not apply in the nonlinear case, when choosing the observer gains some conditions should be considered to guarantee stability. In [20, 22, 23], sufficient conditions to guarantee asymptotic convergence in the nonlinear case are established. These conditions express how fast must the observer convergence be to guarantee closed-loop stability [24].

4.1 AC/DC voltage–source converter

A mathematical model describing the voltage–source converter (VSC) in a rotating d–q reference frame is given by [37]

$$L\dot{i}_d = -Ri_d - L\omega i_q + \eta_d v_{\mathrm{dc}} - v_d \tag{28}$$

$$L\dot{i}_q = -Ri_q + L\omega i_d + \eta_q v_{\mathrm{dc}} - v_q \tag{29}$$

$$C_{\mathrm{dc}}\dot{v}_{\mathrm{dc}} = -\frac{3}{2}(\eta_d i_d + \eta_q i_q) - \frac{v_{\mathrm{dc}}}{R_{\mathrm{L}}} + \frac{p_{\mathrm{L}}}{v_{\mathrm{dc}}} \tag{30}$$

where i_d, i_q are the currents in the d–q reference frame (A), v_d, v_q the voltages in the d–q reference frame (V), v_{dc} the DC bus voltage (V), p_{L} the power delivered, positive sign (or demanded, negative sign) by the DC source (DC load) (W), η_d, η_q the control signals in the d–q reference frame, R_{L} equivalent resistance of the switching loss (Ω), R the coupling transformer resistance (Ω), L the coupling transformer inductance (H) and ω the synchronous frequency (rad/s). In Fig. 2, the schematic electric circuit representing a VSC is shown.

In the following lines, two cases of disturbance and parameter estimations for VSCs are presented. The load power in a VSC can present wide variations, coupling reactor resistance changes due to temperature effects, whereas VSC losses vary according to the operating point or by an internal fault of the converter. Therefore estimating these variables could be very useful for: controllers to reject load power disturbances; adaptation of the VSC parameters or monitoring internal parameters for model identification or with fault detection purposes of the VSC. For these reasons, two estimation cases are introduced. In the first one, the estimation of the load power and the VSC resistance is accomplished, whereas in the second case an estimator of the coupling reactor and loss equivalent resistances is designed.

4.1.1 Power load and resistance estimation: In this case, the proposed technique is used to estimate the load power p_{L} (an external disturbance) and the coupling transformer resistance (a parameter) in a VSC. It is assumed that AC currents and DC voltage are measured. Partition given in (11) is applied to the VSC model (28)–(30) plus a dynamical extension of the variables to be estimated, yielding

$$\mathbf{x}_a = \begin{bmatrix} i_d & i_q & v_{\mathrm{dc}} \end{bmatrix}^{\mathrm{T}} \tag{31}$$

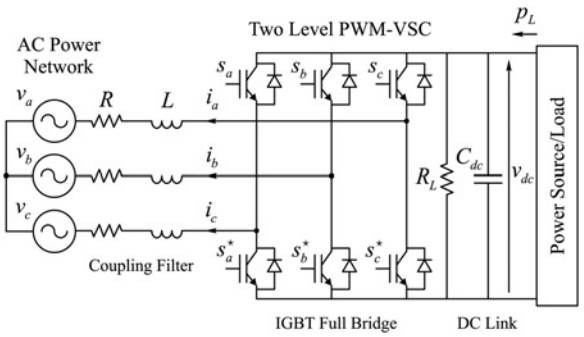

Figure 2 *Electrical circuit of a three-phase AC/DC VSC*

$$\mathbf{x}_b = \begin{bmatrix} p_{\mathrm{L}} & R \end{bmatrix}^{\mathrm{T}} \tag{32}$$

$$\mathbf{u} = \begin{bmatrix} \eta_d & \eta_q \end{bmatrix}^{\mathrm{T}} \tag{33}$$

where in this case

$$\mathbf{N} = \begin{bmatrix} 0 & -\omega & \dfrac{\eta_d}{L} \\ \omega & 0 & \dfrac{\eta_q}{L} \\ -\dfrac{3\eta_d}{2C_{\mathrm{dc}}} & -\dfrac{3\eta_q}{2C_{\mathrm{dc}}} & \dfrac{-1}{C_{\mathrm{dc}}R_L} \end{bmatrix}$$

$$\mathbf{M} = \begin{bmatrix} 0 & -\dfrac{i_d}{L} \\ 0 & -\dfrac{i_q}{L} \\ \dfrac{1}{C_{\mathrm{dc}}v_{\mathrm{dc}}} & 0 \end{bmatrix} \tag{34}$$

$$\mathbf{R} = \mathbf{0}^{2\times 3}, \quad \mathbf{S} = \mathbf{0}^{2\times 2}$$

$$\mathbf{g}_a = \begin{bmatrix} -\dfrac{v_d}{L} & -\dfrac{v_q}{L} & 0 \end{bmatrix}^{\mathrm{T}}, \quad \mathbf{g}_b = \mathbf{0}^{2\times 1}$$

Consequently, the estimation error dynamics, characterised by $\mathbf{A}_r$ in equation (21), becomes

$$\mathbf{A}_r = \mathbf{S} - \mathbf{G}\frac{\partial \mathbf{T}}{\partial \mathbf{x}_a}\mathbf{M} = \begin{bmatrix} -\dfrac{\lambda_1}{C_{\mathrm{dc}}v_{\mathrm{dc}}}\dfrac{\partial w_1}{\partial v_{\mathrm{dc}}} & \lambda_1\left(\dfrac{i_d}{L}\dfrac{\partial w_1}{\partial i_d} + \dfrac{i_q}{L}\dfrac{\partial w_1}{\partial i_q}\right) \\ -\dfrac{\lambda_2}{C_{\mathrm{dc}}v_{\mathrm{dc}}}\dfrac{\partial w_2}{\partial v_{\mathrm{dc}}} & \lambda_2\left(\dfrac{i_d}{L}\dfrac{\partial w_2}{\partial i_d} + \dfrac{i_q}{L}\dfrac{\partial w_2}{\partial i_q}\right) \end{bmatrix}$$

where $\mathbf{G} = \mathrm{diag}([\lambda_1\ \lambda_2])$ was chosen as the gain matrix of the observer. By equaling the above equation with a constant matrix, the following PDE system is obtained

$$-\frac{\lambda_1}{C_{\mathrm{dc}}v_{\mathrm{dc}}}\frac{\partial w_1}{\partial v_{\mathrm{dc}}} = -\lambda_1 \tag{35}$$

$$\lambda_1\left(\frac{i_d}{L}\frac{\partial w_1}{\partial i_d} + \frac{i_q}{L}\frac{\partial w_1}{\partial i_q}\right) = 0 \tag{36}$$

$$-\frac{\lambda_2}{C_{\mathrm{dc}}v_{\mathrm{dc}}}\frac{\partial w_2}{\partial v_{\mathrm{dc}}} = 0 \tag{37}$$

$$\lambda_2\left(\frac{i_d}{L}\frac{\partial w_2}{\partial i_d} + \frac{i_q}{L}\frac{\partial w_2}{\partial i_q}\right) = -\lambda_2 \tag{38}$$

This PDE system can be solved in different ways. A commercial software, for instance, MAPLE™ can be employed. The solution to (35)–(38) results in the following output transformation

$$\mathbf{w} = \mathbf{T}(\mathbf{x}_a) = \begin{bmatrix} w_1 \\ w_2 \end{bmatrix} = \begin{bmatrix} \dfrac{1}{2}C_{\mathrm{dc}}v_{\mathrm{dc}}^2 \\ -\dfrac{1}{2}L\ln(i_d^2 + i_q^2) \end{bmatrix} \tag{39}$$

Therefore the observer dynamical structure (25) is

$$\dot{\xi}_1 = -\lambda_1\left(\xi_1 + v_{\mathrm{dc}}\left(-\frac{3}{2}(i_d\eta_d + i_q\eta_q) - \frac{v_{\mathrm{dc}}}{R_{\mathrm{L}}} + \frac{\lambda_1 C_{\mathrm{dc}}v_{\mathrm{dc}}}{2}\right)\right)$$

$$\dot{\xi}_2 = \lambda_2\left(-\xi_2 + \frac{(i_d\eta_d + i_q\eta_q)v_{\mathrm{dc}} - i_d v_d - i_q v_q}{i_d^2 + i_q^2} + \frac{\lambda_2 L}{2}\ln(i_d^2 + i_q^2)\right)$$

and the estimated variables are recovered by using (26)

$$\hat{p}_L = \xi_1 + \frac{1}{2}\lambda_1 C_{\mathrm{dc}}v_{\mathrm{dc}}^2 \tag{40}$$

$$\hat{R} = \xi_2 - \frac{1}{2}\lambda_2 L\ln(i_d^2 + i_q^2) \tag{41}$$

Due to that transformation (39) was used, the estimation error dynamics (27) becomes

$$\dot{\mathbf{e}} = \mathbf{A}_r\mathbf{e} = -\begin{bmatrix} \lambda_1 & 0 \\ 0 & \lambda_2 \end{bmatrix}\mathbf{e} \tag{42}$$

where $\mathbf{e} = \begin{bmatrix} (p_L - \hat{p}_L) & (R - \hat{R}) \end{bmatrix}^{\mathrm{T}}$ is the estimation error vector in original coordinates. Note that a decoupled and linear dynamics is attained. In this way, the possibility of peaking phenomenon is avoided [36].

In order to illustrate the convergence of the estimation error the following test was carried out. It was considered the VSC parameters given in [13] and the load power was varied from 20 to 10 kW at 0.04 s. Then, at 0.14 s the resistance is increased to 0.6 Ω. Figs. 3*a* and *b* show the actual values of load power and resistance and their estimates. It is clearly seen that the convergence is exponential in the original coordinates and decoupled. Note that the VSC currents have transient oscillations when disturbances appear (Fig. 3*c*). However, these oscillations do not affect the exponential convergence of the estimated variables.

4.1.2 Resistance and loss equivalent resistance estimation: By employing the proposed procedure such as in the above case, the resistance and loss equivalent resistance can be estimated. In this case, the output

doi: 10.1049/iet-cta.2009.0095

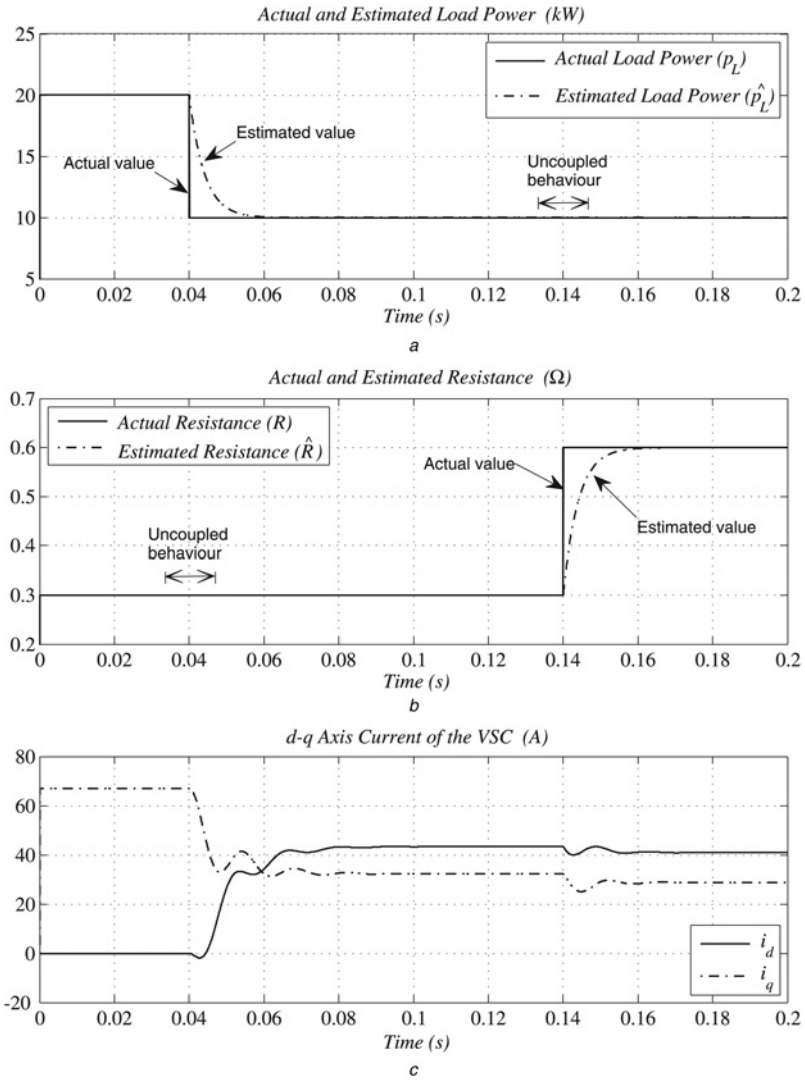

Figure 3 *Exponential and decoupled convergence of*
a Load power
b Resistance
c *d*–*q* axis VSC currents

transformation is given by

$$\mathbf{w} = \mathbf{T}(\mathbf{x}_a) = \begin{bmatrix} w_1 \\ w_2 \end{bmatrix} = \begin{bmatrix} -\frac{1}{2}L\ln(i_d^2 + i_q^2) \\ -C_{\mathrm{dc}}\ln v_{\mathrm{dc}} \end{bmatrix} \tag{43}$$

Note that in both cases the transformations (39) and (43) are hard to obtain in an intuitive way; for this reason, the systematic technique presented in this paper is very useful for designers.

4.2 Magnetic levitation system

A simplified description of a magnetic levitation system (MLS) is given by [38]

$$\dot{i} = \frac{R}{k}(x - c)i - \frac{vi}{(c - x)} + \frac{(c - x)}{k}u_e \tag{44}$$

$$\dot{x} = v \tag{45}$$

$$\dot{v} = \frac{k}{2m}\frac{i^2}{(c - x)^2} - g \tag{46}$$

where i is the current of the MLS electrical circuit (A), u_e the voltage of the MLS electrical circuit (V), x the levitating piece position (m), v the levitating piece speed (m/s), R the winding resistance (Ω), m the mass of the levitating piece (kg), c the nominal position of the levitating piece (m), k the constant that depends on the number of coil turns and g the gravity acceleration (m/s^2). These variables are shown in Fig. 4.

Assume that the electrical resistance (a parameter) is to be estimated. A nonlinearity results from the multiplication between current and position states and the parameter to be estimated.

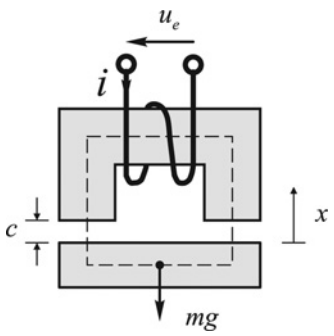

Figure 4 *Schematic of the MLS*

The matrix $\mathbf{A}_r$ results

$$\mathbf{A}_r = \mathbf{S} - \mathbf{G}\frac{\partial \mathbf{T}}{\partial \mathbf{x}_a}\mathbf{M} = -\lambda \frac{(x-c)i}{k}\frac{\partial w}{\partial i} \tag{47}$$

where the scalar gain $\mathbf{G} = \lambda$ is selected. Then, the output transformation obtained by solving (47) becomes

$$w = T(\mathbf{x}_a) = \frac{k \ln i}{(x-c)} \tag{48}$$

In this way, the linear estimation error dynamics (27) results

$$\dot{e} = \mathbf{A}_r e = -\lambda e \tag{49}$$

which is obtained by using the output transformation given by (48). Again the methodology gives a non-trivial output transformation w, accomplishing an exponentially error dynamics in the original coordinates, where convergence rate is chosen by the design parameter λ.

In electromagnetic cranes, the mass of the levitating piece is generally unknown or it can vary during the suspension time. For this reason, the proposed technique is applied in order to estimate the mass of the levitating piece. In this way, the estime can be used for tuning the crane control or for monitoring purposes. Proceeding as in the above cases, the matrix $\mathbf{A}_r$ results

$$\mathbf{A}_r = \mathbf{S} - \mathbf{G}\frac{\partial \mathbf{T}}{\partial \mathbf{x}_a}\mathbf{M} = -\lambda \frac{ki^2}{2(x-c)^2}\frac{\partial w}{\partial v} \tag{50}$$

whereas the output transformation obtained by solving (50) becomes

$$w = T(\mathbf{x}_a) = \frac{2v(x-c)^2}{ki^2} \tag{51}$$

The performance and behaviour of the levitating piece mass estimator are depicted in the following test. Parameters of the MLS presented in [38] were chosen. At the beginning, the MLS is in equilibrium when at $t = 0.05$ s, a 50% loss of the levitating piece mass occurs. In Fig. 5*a* actual and estimated mass are shown. There, it can be seen the exponential convergence of the estimator. In Fig. 5*b* the estimation error is drawn. The winding current and the levitating piece position are shown in Figs. 5*c* and *d*.

4.3 Permanent magnet synchronous machine

The permanent magnet synchronous machine (PMSM) model is described in rotating reference frame by the following equations [39]

$$L_d \dot{i}_d = -Ri_d - N_r \omega L_q i_q - v_d \tag{52}$$

$$L_q \dot{i}_q = -Ri_q + N_r \omega L_d i_d + N_r \omega \Psi_{\mathrm{m}} - v_q \tag{53}$$

$$J\dot{\omega} = T_{\mathrm{m}} - T_{\mathrm{e}} - D_b \omega \tag{54}$$

with

$$T_{\mathrm{e}} = \frac{3N_r}{2}(\Psi_{\mathrm{m}} i_q + (L_d - L_q) i_d i_q) \tag{55}$$

where i_d and i_q are the stator currents in the d–q axis (A), v_d and v_q the stator voltages in the d–q axis (V), ω the rotor speed (rad/s), R the stator winding resistance (Ω), L_d and L_q the d–q inductances of the stator winding (H), Ψ_{m} the magnetic flux (Nm/A), J the rotor inertia (kgm^2), D_b the viscous friction constant (Nms/rad), N_r the number of pair poles, T_{m} the mechanical load torque (Nm) and T_{e} the electrical torque (Nm). The schematic circuit of a PMSM is shown in Fig. 6.

In a motor, the load torque can present large variations, the stator resistance can vary due to temperature changes and the permanent magnet flux can change because of demagnetisation effects. Thus, different estimations of these variables are very useful when it is needed to construct controllers for rejecting load torque disturbances, monitoring of the internal parameters or to build algorithms with fault detection purposes. By keeping in mind the above mentioned, two estimators are presented. First, an estimator for the load torque and the stator resistance is designed. Then, a second estimator which can detect the magnetic flux of the PMSM is built.

4.3.1 Load torque and stator resistance estimation: By applying the proposed method, the load torque and the stator resistance can be estimated. Therefore proceeding in a manner similar to the previous examples, we can find that the output transformation is given by

$$\mathbf{w} = \mathbf{T}(\mathbf{x}_a) = \begin{bmatrix} w_1 \\ w_2 \end{bmatrix} = \begin{bmatrix} -\frac{1}{2}L \ln(i_d^2 + i_q^2) \\ J\omega \end{bmatrix} \tag{56}$$

where a round rotor ($L \triangleq L_d = L_q$) was assumed.

doi: 10.1049/iet-cta.2009.0095

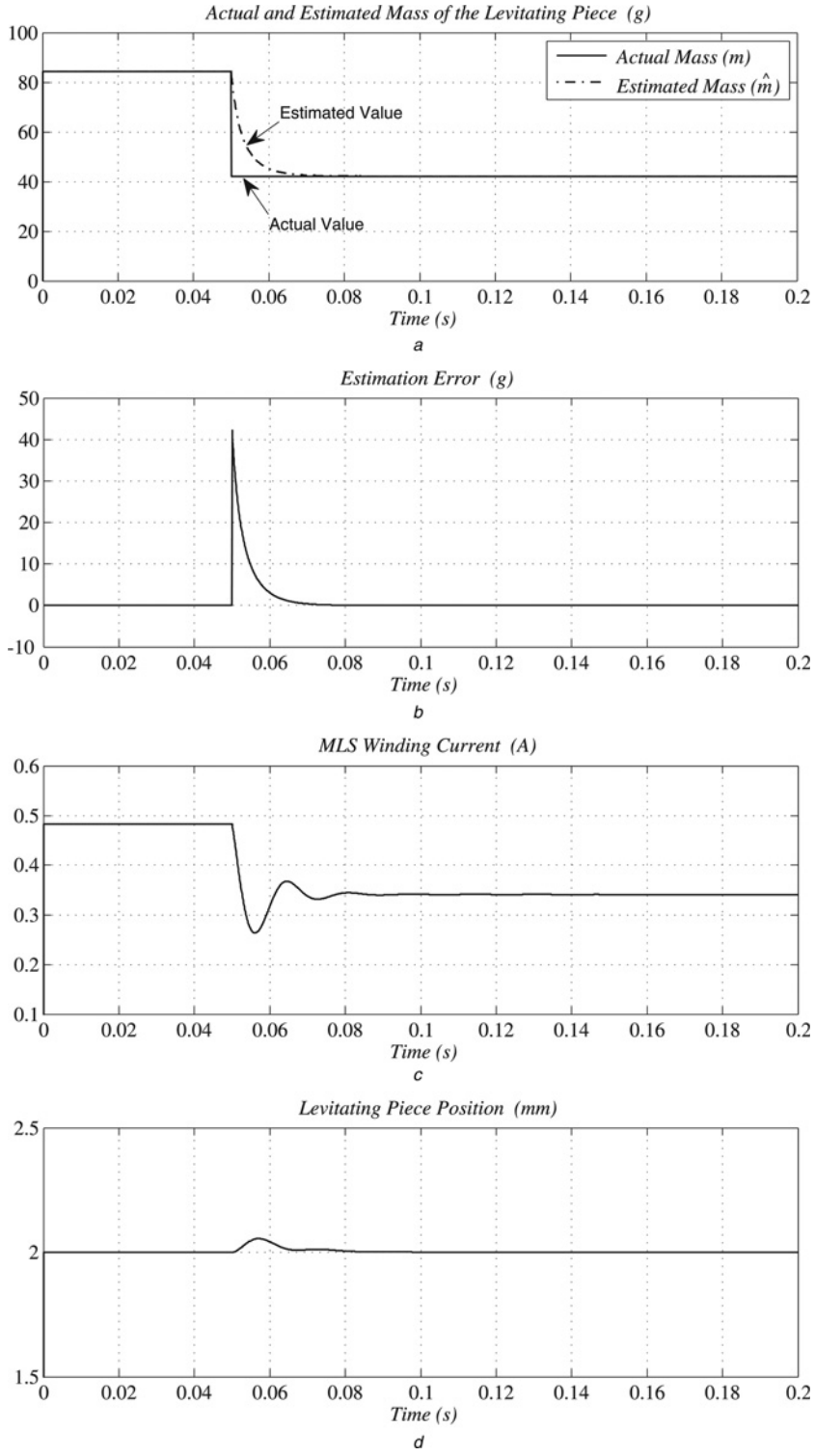

Figure 5 *Mass change test in the MLS*

a Exponential convergence of the levitating piece mass
b Estimation error
c MLS winding current
d Levitating piece position

This transformation is similar to the used in the VSC resistance estimation case. However, a less intuitive transformation appears when the permanent magnet flux is to be estimated. This case is developed in what follows.

4.3.2 Magnetic flux estimation: The permanent magnet flux in a PMSM can vary (e.g. by either saturation or demagnetisation effects). In this case, it is important to estimate it, for controlling or monitoring purpose [40]. To

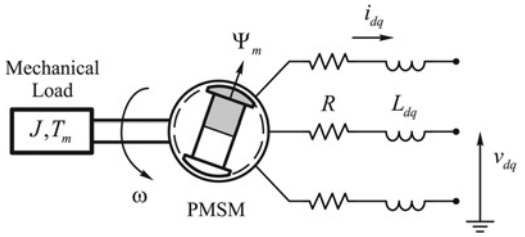

Figure 6 *Schematic circuit of loaded PMSM*

this end, the proposed technique can be utilised. Note that in the PMSM model, the permanent magnet flux constant multiplies two states (one current and rotor speed) in two different equations.

First, (11) is applied to the PMSM model, yielding

$$\mathbf{x}_a = \begin{bmatrix} i_d & i_q & \omega \end{bmatrix}^{\mathrm{T}} \tag{57}$$

$$\mathbf{x}_b = \Psi_m \tag{58}$$

$$\mathbf{u} = \begin{bmatrix} v_d & v_q \end{bmatrix}^{\mathrm{T}} \tag{59}$$

where

$$\mathbf{N} = \begin{bmatrix} -\dfrac{R}{L_d} & -\dfrac{N_r \omega L_q}{L_d} & 0 \\ \dfrac{N_r \omega L_d}{L_q} & \dfrac{-R}{L_q} & 0 \\ \dfrac{-3N_r}{2J}(L_d - L_q) i_q & 0 & -\dfrac{D_b}{J} \end{bmatrix}$$

$$\mathbf{R} = \mathbf{0}^{1\times 3}, \quad \mathbf{M} = \begin{bmatrix} 0 \\ \dfrac{N_r \omega}{L_q} \\ -\dfrac{3N_r}{2J} i_q \end{bmatrix}, \quad \mathbf{S} = 0 \tag{60}$$

$$\mathbf{g}_a = \begin{bmatrix} -\dfrac{v_d}{L_d} & -\dfrac{v_q}{L_q} & \dfrac{T_m}{J} \end{bmatrix}^{\mathrm{T}}, \quad \mathbf{g}_b = 0$$

Then, (21) is represented by

$$\mathbf{A}_r = \mathbf{S} - \mathbf{G}\frac{\partial \mathbf{T}}{\partial \mathbf{x}_a}\mathbf{M} = -\lambda\left(\frac{N_r \omega}{L_q}\frac{\partial w}{\partial i_q} - \frac{3N_r i_q}{2J}\frac{\partial w}{\partial \omega}\right) \tag{61}$$

where the constant $\mathbf{G} = \lambda$ is chosen. By solving (61), the

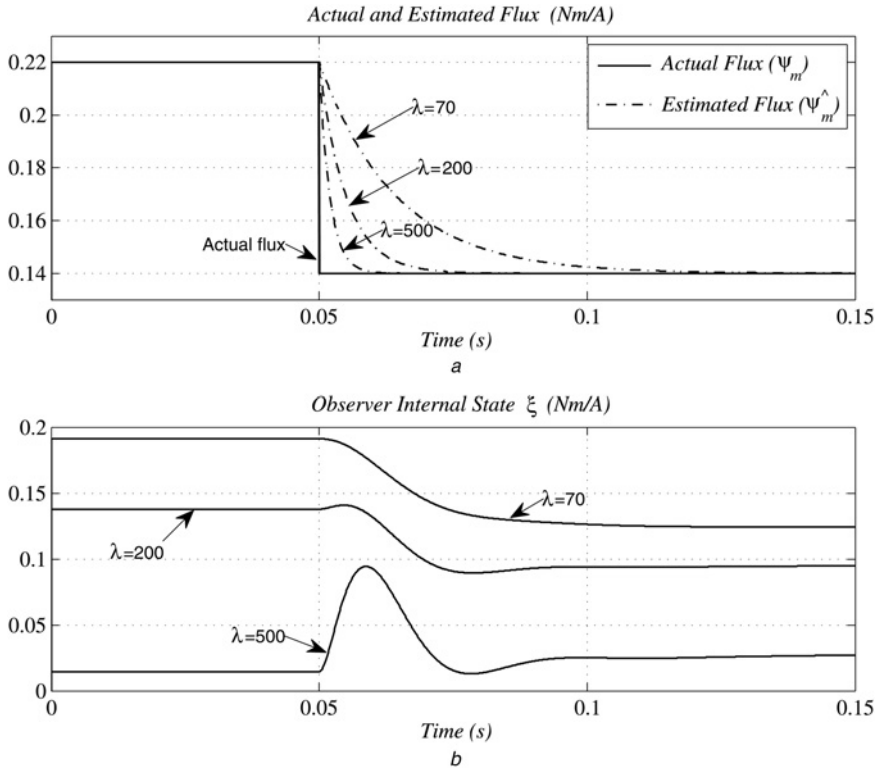

Figure 7 *Exponential convergence of PMSM flux and dynamics of the observer internal state*

a The actual and estimated fluxes for different values of λ
b The dinamical response of the internal state ξ

IET Control Theory Appl., 2010, Vol. 4, Iss. 5, pp. 724–734
doi: 10.1049/iet-cta.2009.0095

following output transformation is obtained

$$w = T(\mathbf{x}_a) = \sqrt{\frac{2JL_q}{3N_r^2}} \arctan\left(\sqrt{\frac{3L_q}{2J}}\frac{i_q}{\omega}\right) \tag{62}$$

Consequently, the estimation error $(e = \Psi_m - \hat{\Psi}_m)$ dynamics converges in an exponential way, given that $\dot{e} = \mathbf{A}_r e = -\lambda e$. The convergence rate is fixed by the selection of the design parameter λ, and as in the above examples, it is independent of the state variables.

In order to show the behaviour of the designed estimator, a test was carried out considering the PMSM presented in [39]. Fig. 7*a* shows the actual and estimated fluxes for different values of λ. It can be seen that the exponential convergence of the estimated flux, when the flux is decreased to 35%. The dynamical response of the internal state ξ is illustrated in Fig. 7*b*.

5 Conclusions

A systematic way to find a reduced-order nonlinear observer with linear error dynamics has been presented. This technique allows us to estimate signals, parameters and disturbances, and it can be used for model-based controllers, feedforward disturbance compensators, variable monitoring and fault detection among others.

Several examples have been introduced to show the behaviour of the observer designed with the proposed methodology. In the introduced applications, the output transformation cannot be found in an intuitive way when linear estimation error dynamics in the original coordinates is to be attained. In such cases, the proposed systematic technique is useful to construct signal estimators.

6 References

[1] LIN F.-J., CHOU P.-H., KUNG Y.-S.: 'Robust fuzzy neural network controller with nonlinear disturbance observer for two-axis motion control system', *IET Control Theory Appl.*, 2008, **2**, (2), pp. 151–167

[2] MAURICIO J.M., LEON A.E., GOMEZ-EXPOSITO A., SOLSONA J.A.: 'An adaptive nonlinear controller for DFIM-based wind energy conversion systems', *IEEE Trans. Energy Conver.*, 2008, **23**, (4), pp. 1025–1035

[3] SIVRIOGLU S.: 'Adaptive backstepping for switching control active magnetic bearing system with vibrating base', *IET Control Theory Appl.*, 2007, **1**, (4), pp. 1054–1059

[4] MUHANDO E.B., SENJYU T., YONA A., KINJO H., FUNABASHI T.: 'Disturbance rejection by dual pitch control and self-tuning regulator for wind turbine generator parametric uncertainty compensation', *IET Control Theory Appl.*, 2007, **1**, (5), pp. 1431–1440

[5] CHEN W., SAIF M.: 'Observer-based strategies for actuator fault detection, isolation and estimation for certain class of uncertain nonlinear systems', *IET Control Theory Appl.*, 2007, **1**, (6), pp. 1672–1680

[6] LIU C.-S., ZHANG S.-J., HU S.-S.: 'Adaptive neural-networks-based fault detection and diagnosis using unmeasured states', *IET Control Theory Appl.*, 2008, **2**, (12), pp. 1066–1076

[7] YAN X.-G., EDWARDS C.: 'Fault estimation for single output nonlinear systems using an adaptive sliding mode estimator', *IET Control Theory Appl.*, 2008, **2**, (10), pp. 841–850

[8] MARINO R., PERESADA S., TOMEI P.: 'Exponentially convergent rotor resistance estimation for induction motors', *IEEE Trans. Ind. Electron.*, 1995, **42**, (5), pp. 508–515

[9] DE LEON-MORALES J., CASTRO-LINARES R., GUEVARA O.H.: 'Observer-based controller for position regulation of stepping motor', *IEE Proc. Control Theory Appl.*, 2005, **152**, (4), pp. 465–476

[10] JAIN A., JOSHI K., BEHAL A., MOHAN N.: 'Voltage regulation with STATCOMs: modeling, control and results', *IEEE Trans. Power Deliv.*, 2006, **21**, (2), pp. 726–735

[11] LIU L., CARTES D.A.: 'Synchronisation based adaptive parameter identification for permanent magnet synchronous motors', *IET Control Theory Appl.*, 2007, **1**, (4), pp. 1015–1022

[12] MARINO R., TOMEI P.: 'Nonlinear control design: geometric, adaptive and robust' (Prentice-Hall, 1995)

[13] LEON A.E., SOLSONA J.A., VALLA M.I.: 'Control of three-phase voltage-source converters with reduced number of sensors'. 34th Annual Conf. IEEE Industrial Electronics, IECON'08, November 2008, pp. 641–646

[14] GHANES M., DE LEON J., GLUMINEAU A.: 'Cascade and high-gain observers comparison for sensorless closedloop induction motor control', *IET Control Theory Appl.*, 2008, **2**, (2), pp. 133–150

[15] KAMAS L.A., SANDERS S.R.: 'Parameter and state estimation in power electronic circuits', *IEEE Trans. Circuits Syst. I, Fundam. Theory Appl.*, 1993, **40**, (12), pp. 920–928

[16] LEE T.-S., TZENG K.-S.: 'Input–output linearizing control with load estimator for three-phase AC/DC voltage-source converters'. IEEE 33rd Power Electr. Spec. Conf., PESC'02, June 2002, vol. 2, (4), pp. 791–795

[17] GENSIOR A., WOYWODE O., RUDOLPH J., GULDNER H.: 'On differential flatness, trajectory planning, observers, and stabilization for DC–DC converters', *IEEE Trans. Circuits Syst. I, Fundam. Theory Appl.*, 2006, **53**, (9), pp. 2000–2010

[18] GENSIOR A., SIRA-RAMIREZ H., RUDOLPH J., GULDNER H.: 'On some nonlinear current controllers for three-phase boost rectifiers', *IEEE Trans. Ind. Electron.*, 2009, **56**, (2), pp. 360–370

[19] OGATA K.: 'Modern control engineering' (Prentice-Hall, 1997, 3rd edn.)

[20] ESFANDIARI F., KHALIL H.K.: 'Output feedback stabilization of fully linearizable systems', *Int. J. Control*, 1992, **56**, pp. 1007–1037

[21] TEEL A., PRALY L.: 'Global stability and observability imply semi-global stability by output feedback', *Syst. Control Lett.*, 1994, **22**, pp. 313–325

[22] TEEL A., PRALY L.: 'Tools for semi-global stabilization by partial state output feedback', *SIAM J. Control Optim.*, 1995, **22**, pp. 1443–1488

[23] ETCHECHOURY M., SOLSONA J., MURAVCHIK C.: 'On the stability of nonlinear plants that include an observer for their feedback linearization', *Int. J. Syst. Sci.*, 1996, **27**, pp. 1461–1466

[24] ETCHECHOURY M., SOLSONA J., MURAVCHIK C.: 'Feedback linearization via state transformation using estimated states', *Int. J. Syst. Sci.*, 2001, **32**, (1), pp. 1–7

[25] THAU F.E.: 'Observing the state of nonlinear dynamic systems', *Int. J. Control*, 1973, **17**, (3), pp. 471–479

[26] BESTLE D., ZEITZ M.: 'Canonical form observer for non-linear timevariable systems', *Int. J. Control*, 1983, **38**, pp. 419–431

[27] CICCARELLA G., DALLA MORA M., GERMANI A.: 'A Luenberger-like observer for nonlinear systems', *Int. J. Control*, 1993, **57**, (3), pp. 537–556

[28] MORA M.D., GERMANI A., MANES C.: 'A state observer for nonlinear dynamical systems', *Nonlinear Anal.*, 1997, **30**, (7), pp. 4485–4496

[29] ROBENACK K., LYNCH A.F.: 'High-gain nonlinear observer design using the observer canonical form', *IET Control Theory Appl.*, 2007, **1**, (6), pp. 1574–1579

[30] WALCOTT B.L., CORLESS M.J., ZAK S.H.: 'Comparative study of nonlinear state-observation techniques', *Int. J. Control*, 1987, **45**, pp. 2109–2132

[31] MOUYON PH.: 'Tools for nonlinear observer design'. IEEE Int. Symp. on Diagnostics and Drivers, SDEMPED97, Carry-Le-Rouet, France, September 1997, pp. 1–6

[32] KRENER A.J., ISIDORI A.: 'Linearization by output injection and nonlinear observers', *Syst. Control Lett.*, 1983, **3**, (1), pp. 47–52

[33] KRENER A.J., RESPONDEK W.: 'Nonlinear observers with linearizable error dynamics', *SIAM J. Control and Optim.*, 1985, **23**, (2), pp. 197–216

[34] KAZANTZIS N., KRAVARIS C.: 'Nonlinear observer design using Lyapunov's auxiliary theorem', *Syst. Control Lett.*, 1998, **34**, (5), pp. 241–247

[35] KRAVARIS C., SOTIROPOULOS V., GEORGIOU C., KAZANTZIS N., XIAO M.Q., KRENER A.J.: 'Nonlinear observer design for state and disturbance estimation', *Syst. Control Lett.*, 2007, **56**, (11–12), pp. 730–735

[36] SUSSMANN H.J., KOKOTOVIC P.V.: 'The peaking phenomenon and the global stabilization of nonlinear systems', *IEEE Trans. Autom. Control*, 1991, **36**, (4), pp. 424–440

[37] BLASCO V., KAURA V.: 'A new mathematical model and control of a three-phase AC–DC voltage source converter', *IEEE Trans. Power Electron.*, 1997, **12**, (1), pp. 116–123

[38] RODRIGUEZ H., SIGUERDIDJANE H., ORTEGA R.: 'Experimental comparison of linear and nonlinear controllers for a magnetic suspension'. IEEE Int. Conf. on Control Applications, September 2000, pp. 715–719

[39] SOLSONA J., VALLA M.I., MURAVCHIK C.: 'A nonlinear reduced order observer for permanent magnet synchronous motors', *IEEE Trans. Ind. Electron.*, 1996, **43**, (4), pp. 492–497

[40] WANG S.-J., FANG C.-H., LIN S.-K.: 'A flux estimation method for a permanent-magnet synchronous motor', *J. Magn. Magn. Mater.*, 2004, **282**, (12), pp. 355–359

doi: 10.1049/iet-cta.2009.0095